Design and performance test of the fast-steering mirror with flexure hinge used in vehicle track-launch system*

XU Xin-hang (徐新行)[1]**, **ZHANG Gui-ming** (张贵明)[2], and **CHEN Chang-bo** (陈昌博)[1,3]

1. Changchun Institute of Optics, Fine Mechanics and Physics, Chinese Academy of Sciences, Changchun 130033, China

2. Xuchang College of Vocational Technology, Xuchang 461000, China

3. University of Chinese Academy of Science, Beijing 100049, China

(Received 18 October 2018; Revised 27 November 2018)

To accurately launch laser, a fast-steering mirror (FSM) with flexure hinge is designed. First, actuators, angle sensors and flexure hinge were designed or selected respectively according to requirements of vehicle track-launch system. Then, the servo control system with two closed loops was projected after fine manufacturing and assembling. Finally, the pointing precisions of FSM on the static and vibrancy platforms were tested. The results show that the designed FSM with pointing error range on the static platform is less than 0.9″, and less than 44.5″ on the vibrancy shaker, which can meet the requirements of vehicle track-launch system application.

Document code: A **Article ID:** 1673-1905(2019)03-0179-6

DOI https://doi.org/10.1007/s11801-019-8163-9

Fast-steering mirror (FSM), a precision optical device, is used to precisely control the direction of beam by controlling the position of mirror[1-4]. FSM, with a series of advantages, such as fast response rate, high pointing precision and high angular resolution, has been used in astronomical telescope in a broad sense, laser communication, adaptive optics, high-precision laser combining and composite axis precision tracking[5-8]. In recent years, the research on high-performance FSM has been focused on the structure with flexure hinges at home and abroad, whose outstanding advantages include simple structure, no friction and fast response rate[9-12]. Byoung Uk Nam et al[13] designed a hinge mechanism including double notch hinge and leaf spring for the fast steering mirror of large diameter. Min Liu et al[14] designed a multi-notched flexure hinge for compliant mechanisms. Yongjun Long et al[15] designed a fast steering mirror with flexible diaphragm and axial flexure. Myung Cho et al[16] designed the fast steering secondary mirror with outer spring, center spring and lateral flexure for the Giant Magellan Telescope Shubao Shao et al[17] designed the decoupled 2-DoF flexure hinge for two-degree-of-freedom piezo-driven fast steering mirror[18]. However, anti-vibration performance of FSM with flexure hinge is relatively limited[18-20]. In the vehicle track-launch system, the high-frequency vibration caused by engine and power station, and the disturbance caused by the road bumps were unavoidable. Though some shock absorbers were used in the system, the vibration still cannot be eliminated completely. To adapt to vibration conditions of the vehicle track-launch system required to work during travelling, an FSM with high precision and high environmental adaptability was in urgent needs in terms of insuring emission lasers accurately hit aero target and destroy or interfere enemy detector.

The structure principle diagram of FSM with flexure hinge is shown in Fig.1. The FSM was mainly composed of mirror, mirror holder, flexible hinge, support base, voice coil motors and angle sensors. To furthest decrease moving parts inertia of FSM, the motor coils were selected as motion parts of FSM, and the magnets of motor were selected as static parts of FSM due to that the weight of the coil is around 1/4 time of the magnet. A flexure hinge at the center of FSM mechanical structure connected motion parts of FSM to the static parts.

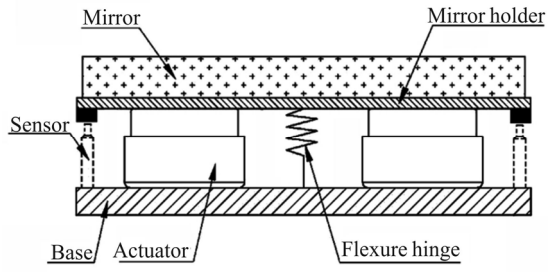

Fig.1 Principle diagram of FSM with flexure hinge

According to the application requirements of the

* This work has been supported by the Program of Science and Technology Development Plan of Jilin Province (No.20180520185JH).

** E-mail: xxh123321xxh@163.com

Vehicle photoelectric track-launch system and characteristics of the laser beam, the main performance indexes of FSM were determined as shown in Tab.1.

Tab.1 Performing requirements of FSM

Item	Requirement
Optic diameter	≥Φ75 mm
Maximum angular range	≥±5 mrad (*X*, *Y* axis)
Resonance frequency	≥160 Hz
Pointing error range on the static platform	≤1″
Pointing error range on the vibrancy platform	≤50″

Currently, the common driving elements of FSM are piezoelectric actuator and voice coil motor. The piezoelectric actuators are widely used to manufacture FSM by virtue of its advantages of small volume, large output force and fast response rate. However, its stroke is only a few micrometers to tens of micrometers, and its hysteresis is ineluctable. And the worst of all, the piezoelectric actuator are too crunchy to resist shear stress, even slight shear during installation. Therefore, it is scarcely used in the vehicular environment where the impact and vibration are severe.

The voice coil motor with the advantages of low driving voltage, large stroke, and excellent environmental adaptability, is being frequently used to drive FSM. Fig.2(a) shows the structure size diagram of selected linear voice coil motor in this study, in which the coil of motor was located in the magnet. When the motor was energized, the coil will be suspended in the magnet, and there was a necessary working gap between them. Consequently, when the linear motion was output, there was no friction between coil and magnet, in addition, the coil was allowed to tilt a small angle relative to the magnet.

In this study, 4 voice coil motors were used to provide linear power for FSM. The position of 4 actuators is shown in Fig.2(b). It was beneficial not only to adjust gravity center of FSM moving parts to rotation center, so that FSM movement became more stable, but also to ensure FSM sufficient driving torque. However, higher precision of processing, assembling and controlling was required because of the hyper degrees of freedom structure, and there were two actuators in each dimension and rotation center of FSM was fixed.

Currently, the non-contacting measuring elements used for FSM mainly include capacitance sensor and eddy current sensor. Their technical principle is similar, and volume is very small as well as measurement accuracy. However, the capacitance sensor not only has the shortcoming of temperature drift, but also requires a clean environment, hence it is not suitable for application in the vehicle system with poor conditions. The eddy current sensor has fast response speed, high measurement resolution and excellent environmental adaptability, and furthermore, it can maintain stable measurement accuracy in the −40 °C to +85 °C. In addition, currently indigenous eddy current sensor is becoming increasingly mature. Compared with the high-accuracy capacitance sensor relying on import, it was more adopted into domestic FSM products since the cost of eddy current sensor is lower. In this study, a differential eddy current sensor with four channels was used to measure FSM real-time position. The measurement noise was restrained by averaged data from each two channels, hence higher measurement precision shall be obtained. The main performance parameters of the selected eddy current sensor are shown in Tab.2.

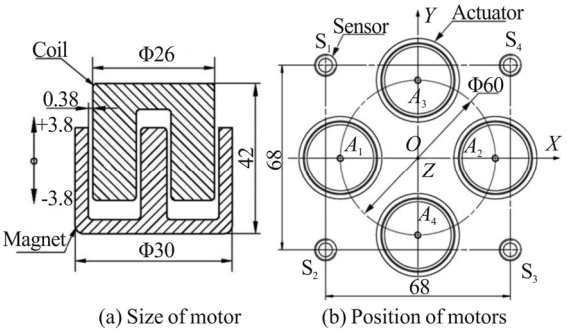

Fig.2 Linear voice coil motors

Tab.2 Performances of eddy current sensor

No.	Items	Value
1	Probe size	M8×40 mm
2	stroke	±0.25 mm
3	response frequency	0—20 kHz
4	resolution	0.1 μm

As shown in Fig.2(b), the four probes of eddy current sensor are arranged on the angle bisector of *X* and *Y* axes in proper sequence since FSM tilting angle in each dimension was obtained by twice averaging measurement data of four sensors, thus maximally compressing volume of FSM and effectively improving measurement precision to FSM. The measurement principle is shown in Fig.3.

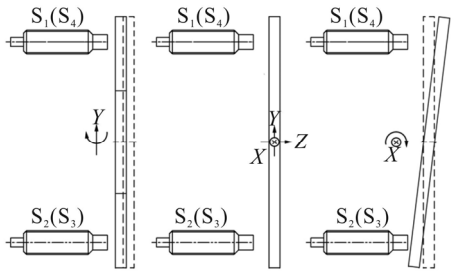

Fig.3 Position of eddy current sensors

The calculation process of FSM tilting angle in each dimension was as below:

$$L_1=\frac{S_1+S_3}{2}, \tag{1}$$

$$L_2=\frac{S_2+S_4}{2}, \tag{2}$$

$$S_P=\frac{L_1+L_2}{2}, \tag{3}$$

$$S_A=\frac{L_1-L_2}{2}, \tag{4}$$

$$\theta_P=\frac{S_P}{r}=\frac{L_1+L_2}{2r}, \tag{5}$$

$$\theta_A=\frac{S_A}{r}=\frac{L_1-L_2}{2r}, \tag{6}$$

where S_1—S_4 are the measured data of each eddy current sensor, L_1 is measurement result of the first group of sensors (S_1, S_3), L_2 is measurement result of the second group of sensors (S_2, S_4), S_P is the displacement of mirror in the sensor position when FSM rotating around the X axis, S_A is the displacement of mirror in the sensor position when FSM rotating around the Y axis, r is the distance from sensor probe to X or Y axis, θ_P is rotating angle of FSM around X axis, and θ_A is rotating angle of FSM around Y axis.

To ensure control bandwidth of FSM high enough, resonant frequency of FSM mechanical structure is required to be higher than working bandwidth of FSM. However, since the driving torque of motor was limited and there was control system in the working direction of FSM, the common design concept is to ensure that the resonant frequency of FSM in the non-working direction is much higher than working bandwidth of system, and the higher the better, while the resonant frequency of FSM in the working direction is much lower than working bandwidth of system, and the lower the better. That is, the first mode and second mode of flexure hinge should be as low as possible, and the third mode and above mode should be as high as possible.

The designed flexure hinge, which is mainly composed of an immobile part, a middle part and a mobile part, is as shown in Fig.4. The immobile part was connected with the supporting base of FSM and the mobile part was connected with the mirror holder of FSM. When FSM rotated around X axis, the mobile part of flexure hinge tilted a small angle by material elastic deformation. FSM rotated around Y axis, the middle part and the mobile part of flexure hinge tilted a small angle synchronously.

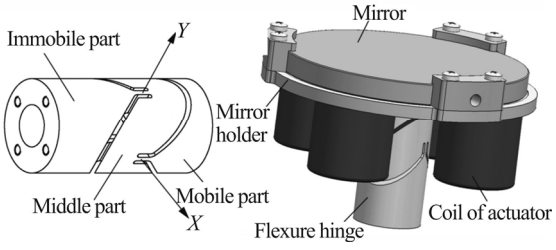

Fig.4 Structure of flexure hinge

After finishing structure of flexure hinge design, its modes and stiffness were simulated by finite element method. Fig.5 shows the analysis results of the 1st to 3rd mode shapes and modes of FSM. It can be found out from Fig.5 that the 1st and 2nd mode shapes are in the working directions of FSM, and the corresponding modes were: M_1=76.3 Hz, M_2=77.6 Hz, which met the design requirements of $f_c>2M_1$, $f_c>2M_2$. The third mode is in the non-working direction of FSM, and the corresponding mode is M_3=382.9 Hz, which met the design requirements of $M_3>2f_c$. f_c is the control bandwidth of FSM system.

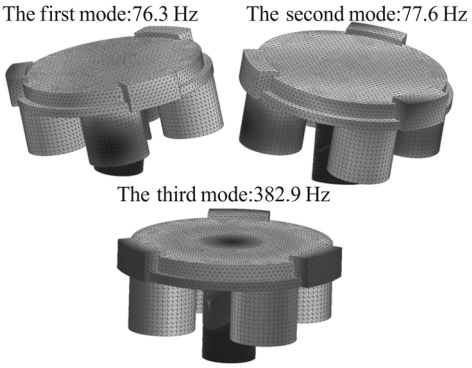

Fig.5 Vibration model analysis results of FSM

The stiffness analysis results of flexure hinge in the working direction are shown in Fig.6. When a torque of 0.86 Nm was applied to working directions of FSM, the maximum displacements of mirror at X-axis and Y-axis are 0.577 mm and 0.575 mm, respectively. The stiffness of the flexure hinge was calculated as: K_x=37.8 Nm/rad and K_y=37.2 Nm/rad.

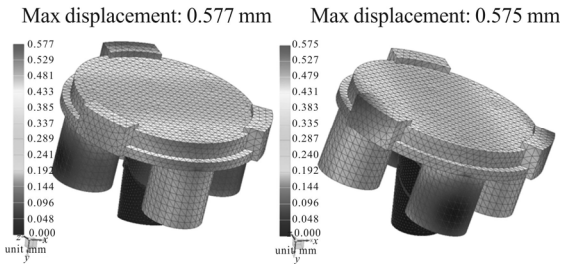

Fig.6 Stiffness analysis results of flexure hinge

The control system of FSM consisted of azimuth and pitch closed-loop systems, and which were the same but independent with respectively. Both of them adopted double closed-loop control mode in which the velocity loop was the inner loop and the position loop was the outer loop. The feedback signals of the position loop was directly provided by the eddy current sensors, while the feedback signals of the velocity loop was obtained from differentially processing to measurement values of sensors. Fig.7 is the principle diagram of FSM control system.

After completing fine manufacturing and assembling of FSM, FSM was manufactured as shown in Fig.8. The actual optical aperture of FSM is Φ80 mm. The maximal

angle stroke is ±6 mrad (*X* and *Y* axis). The stroke is adjustable. The control bandwidth of system is about 200 Hz, which can meet the requirement indexes of FSM.

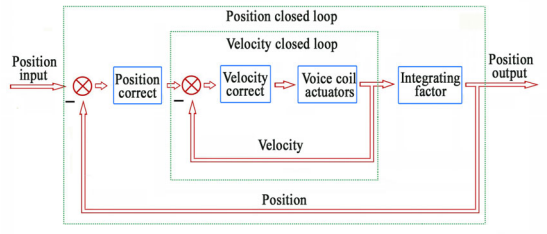

Fig.7 Diagram of servo control system

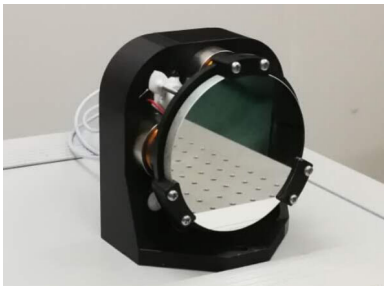

Fig.8 Photograph of FSM with flexure hinge

The autocollimator from Jiujiang Jingda Measurement Technology Co. Ltd whose type is CZS-1A and testing precision is 0.1″, was used to test pointing precision of FSM. The test rig is shown in Fig.9. The test procedures are as follows. a) FSM was positioned at (0″, 0″) by the computer, and then the autocollimator was adjusted to be collimated with FSM. b) FSM was postioned to (100", 100"), while the actual pointing position of FSM was measured by the autocollimator. c) The pointing precision of FSM on the static platform was obtained by analyzing the testing data.

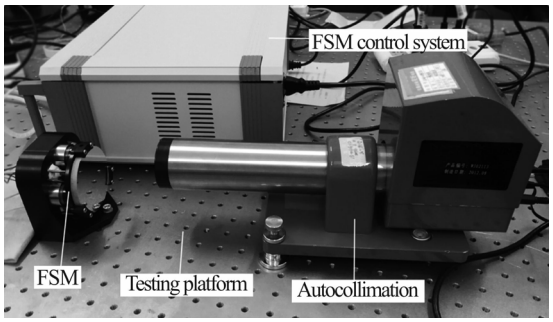

Fig.9 Test rig for FSM pointing precision on the static platform

The testing data on pointing precision of FSM on the static platform are shown in Fig.10. The results show that the pointing error range of FSM in the azimuth direction is no more than 0.5″, and the root mean square (RMS) error is about 0.1″. The pointing error range in the pitch direction is no more than 0.9″, and the RMS error is about 0.2″.

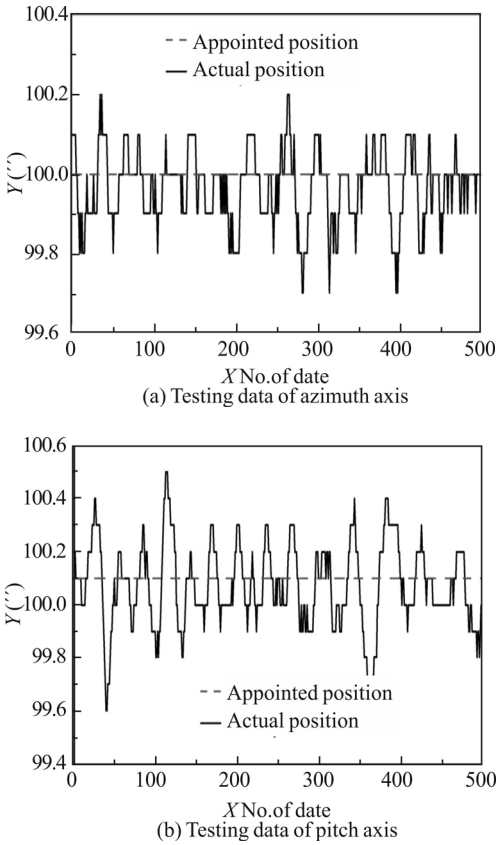

Fig.10 Test results of FSM pointing precision on the static platform

Since the designed fast steering mirror system is used on the vehicle and it is required to work during travelling, which is greatly different from conventional fast steering mirror used static platform generally. The pointing precision of FSM in the vibration environment was tested by collecting data of sensors after special designing of key constituent units, and the test rig is shown in Fig.11. The testing steps are as follows.

a) FSM was fixed on the electrodynamic vibration shaker, ensuring that the working direction of FSM was consistent with the vibration direction of shaker.

b) The vibration shaker was started, the vibration frequency was swept from 1 Hz to 2 000 Hz, and the peak acceleration of random vibration was 1 g.

c) FSM was positioned to (100", 100"), while signals of eddy current sensors were collected.

d) The pointing precision of FSM in specific vibration conditions was obtained by analyzing the collected sensor data.

The testing data on the pointing precision of FSM in the vibration environment are shown in Fig.12. The results demonstrated that the pointing error range of FSM in the azimuth direction is no more than 41.5″, and the RMS error is about 7.5″. The pointing error range in the pitch direction is no more than 44.5″, and the RMS error

is about 7.8″.

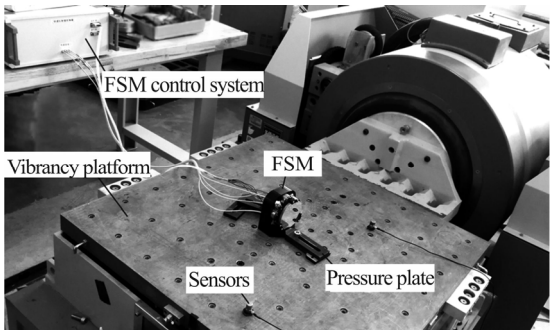

Fig.11 Test rig for pointing precision of FSM in the vibrancy conditions

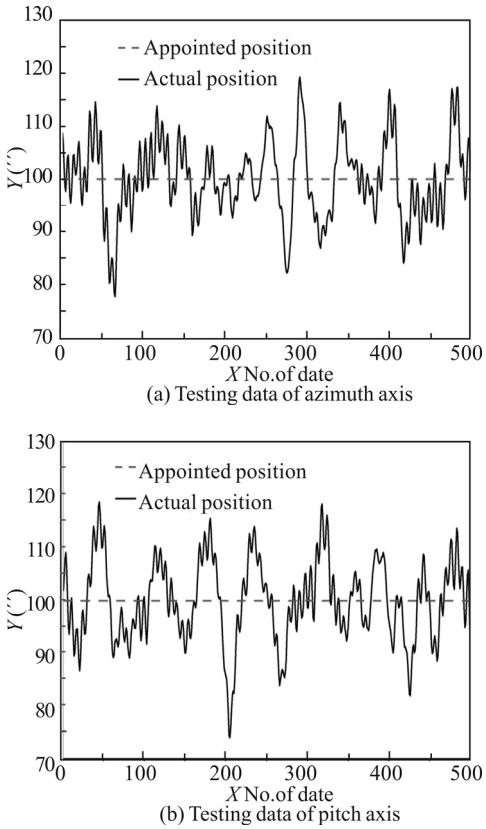

Fig.12 Detection results of FSM pointing precision in the vibrancy conditions

In this paper, the detailed design of FSM with flexure hinge was made according to application requirements of vehicle track-launch system. The differential eddy current sensors with four channels were used for real-time monitoring of the position of FSM, and its measurement noise of the sensors was retained by twice averaging, which effectively ensured the measurement precision to FSM. The mode and stiffness of flexure hinge were analyzed by finite element method. On the basis of ensuring lower resonant frequency of FSM in the working direction, the resonant frequency of FSM in the non-working direction was improved as much as possible, it was beneficial to improve control bandwidth of system. The pointing precisions of FSM on the static platform and in vibration conditions were finally tested respectively. The results show that pointing precision of FSM can meet the application requirements of the vehicle track-launch system.

References

[1] G. Aigouy, K. Benoit, E. Betsch, T. Maillard, M. Fournier and F. Claeyssen, Development of Magnetic Fast Steering Mirror Prototype for Optical Pointing Applications, 16th International Conference on New Actuators, 559 (2018).

[2] Zhichao Dong, Aimin Jiang, Yanfeng Dai and Jianwei Xue, Applied Optics **57**, 9307 (2018).

[3] Ernst Csencsics, Johannes Schlarp and Georg Schitter. High-Performance Hybrid-Reluctance-Force-Based Tip/Tilt System: Design, Control and Evaluation, IEEE/ASME Transactions on Mechatronics, 2494 (2018).

[4] Mei Rong, Hu Zhong-wen, Xu Teng and SUN Chang-sheng, Chinese Astronomy and Astrophysics **42**, 475 (2018).

[5] Li Xian-tao, Zhang Xiao-pei, Mao Da-peng and Sun Jing-hui, Optics and Precision Engineering **25**, 2428 (2017). (in Chinese)

[6] N. Jacka, W. Walker, M. Roybal and J. McNally, Design and qualification of a small customizable fast steering mirror (FSM) for FSOC stabilization and scanning applications, Proceedings of SPIE **10524**, 1052407 (2018).

[7] Wang Wan-ting, Guo Jin, Fang Chu, Jiang Zhen-hua and Wang Ting-feng, Optoelectronics Letters **12**, 426 (2016).

[8] Salim Ibrir, Chun-Yi Su, Boon S. Ooi and M. Slim Alouini, Fast and Reliable Control of Steering Mirrors with Application to Free-Space Communication, International Conference on Advanced Mechatronic Systems, 483 (2017).

[9] Hei Mo, Zhang Lian-chao, Zhou Qing-kun, Lu Ya-fei and Fan Da-peng, J. Cent. South Univ. **22**, 150 (2015).

[10] Li Yao, Wu Hong-tao, Yang Xiao-long, Kang Sheng-zheng and Cheng Shi-li, Optics and Precision Engineering **26**, 1370 (2018). (in Chinese)

[11] Jing Tian, Wenshu Yang, Zhenming Peng and TaoTang, Optical Engineering **55**, 111602 (2016).

[12] Dong Shi-ze, Guo Kang, Li Xian-ling, Chen Hua-nan and Zhang De-Fu, Chinese Optics **10**, 790 (2017). (in Chinese)

[13] Byoung-Uk Nam, Hakin Gimm, Dongwoo Kang and Daegab Gweon, Optical Engineering **55**, 106120 (2016).

[14] Min Lin, Xianmin Zhang and Sergej Fatikow, Precision Engineering **48**, 292 (2017).

[15] Yongjun Long, Xiaohui Wei, Chunlei Wang, Xin Dai and Shigang Wang, Optical Engineering **53**, 054102 (2014).

[16] Myung Cho, Youra Jun, Christoph Dribusch, JieunRyu, Gary Poczulp, Ming Liang, Sungho Lee, Jeong-Yeol Han, UeejeongJeong, SanghyukKim, Bongkon Moon, Chang-Hee Kim, Yunjong Kim, Chan Park, Byeong-Gon Park, II-Kwon Moon, Chan-Hee Lee, Wongi Lee, Ho-Sang Kim and PaulGardner, Robert Bernier, Frank Groark, Hugo Chiquito, Design of the fast steering secondary mirror assembly for the Giant Magellan Telescope, Proceedings of SPIE **10706**, 1070607 (2018).

[17] Shubao Shao, Zheng Tian, Siyang Song and Minglong Xu, Review of Scientific Instruments **89**, 055003 (2018).

[18] Fang Chu, Guo Jin, Yang Guo-qing, Jiang Zhen-hua,Xu Xin-hang and Wang Ting-feng, Optoelectronics Letters **12**, 333 (2016).

[19] Wei Liu, Kainan Yao, Danian Huang, Xudong Lin, Liang Wang and Yaowen Lv, Optics Express **24**, 13288 (2016).

[20] Yingxue Ni, Jiabin Wu, Xiaogang San, Shijie Gao, Shaohang Ding, Jing Wang and Tao Wang, Optical Engineering **57**, 024110 (2018).